Formic Acid Dissociative Adsorption on NiO(111): Energetics and Structure of Adsorbed Formate

Wei Zhao, [1] Andrew D. Doyle, [2] Sawyer E. Morgan, [3]
Michal Bajdich, [2] Jens K. Nørskov, [2] and Charles T. Campbell* [1,3]

1. Department of Chemistry, University of Washington, Seattle Washington 98195-1700, USA
2. SUNCAT Center for Interface Science and Catalysis, Chemical Engineering, Stanford University, Stanford, California 94305, and SLAC National Accelerator Laboratory, 2575 Sand Hill Road, Menlo Park, California 94025, USA
3. Department of Chemical Engineering, University of Washington, Seattle, Washington 98195, United States

Abstract

The dissociative adsorption of carboxylic acids on oxide surfaces is important for understanding adsorbed carboxylates, which are important as intermediates in catalytic reactions, for the organo-functionalization of oxide surfaces, and in many other aspects of oxide surface chemistry. We present here the first direct experimental measurement of the heat of dissociative adsorption of any carboxylic acid on any single-crystal oxide surface. The enthalpy of the dissociative adsorption of formic acid, the simplest carboxylic acid, to produce adsorbed formate and hydrogen (as a surface hydroxyl) on a (2×2)-NiO(111) surface is measured by single crystal adsorption calorimetry. The differential heat of adsorption decreases with formic acid coverage from 202 kJ/mol to 99 kJ/mol at saturation (0.25 ML). The structure of the adsorbed products is clarified by density functional theory (DFT) calculations, which provide energies in reasonable agreement with the calorimetry. These calculations show that formic acid readily dissociates on both the oxygen and Ni terminations of the octapolar NiO(111) surfaces, donating its acid H to a surface lattice oxygen, while HCOO adsorbs preferentially with bridging-type geometry near the M-O_3/O-M_3 sites. The calculated energetics at low coverages agrees well with experimental data, while larger differences are observed at high coverage (0.25 ML). The large decrease in experimental heat of adsorption with coverage can be brought into agreement with the DFT energies if we assume that both types of octapolar surface terminations (O- and Ni-) are present on the starting surface.

* Corresponding author: charliec@uw.edu, tel. = 206-616-6085

Introduction

Formic acid is a very important feedstock for the modern chemical industry. It is a potential product of CO_2 hydrogenation, possessing a high hydrogen-storage capacity, which is considered as a source of hydrogen for various applications.[1-2] In general, the activation of formic acid molecules to dissociate on metal or metal oxide catalysts is the first step for utilization of HCOOH, which typically forms the adsorbed formate ($HCOO_{ad}$) by breaking the O-H bond, with the abstracted H atom attaching to the surface. Formate itself is a very important intermediate in all oxidation and steam reforming reactions of organic molecules and likely exists whenever CO_2 with H_2 or water are present above a catalyst.[3-5] Larger carboxylic acids are also used for organo-functionalization of oxide surfaces, where they often bind via the deprotonated carboxylate functionality.[6] Therefore, characterization of the energetics of dissociative adsorption of formic acid and adsorbed formate on oxide surfaces is obviously crucial for the fundamental understanding of a wide variety of surface reactions and catalytic processes on oxide surfaces. Nevertheless, the heat of the dissociative adsorption has never been reported for formic acid nor any other a carboxylic acid on any single-crystalline oxide surface. Here we report the calorimetric heat of adsorption of the simplest carboxylic acid, HCOOH, on a NiO(111) surface and characterize the resulting formate and hydroxyl structures using DFT. The heats of formic acid dissociative adsorption onto Pt(111)[7] or Ni(111)[8] have been directly measured using single crystal adsorption calorimetry (SCAC) by this group.

Compared to metal surfaces, much less is understood about the chemistry of oxide surfaces, though they play crucial roles in catalysis. While the adsorption energies are known for many species which are molecularly absorbed on well-defined, single-crystal oxide surfaces, only a few values have been reported for dissociatively adsorbed species, where the adsorption energy was estimated based on temperature programmed desorption (TPD) of the reverse process (associative desorption), and a pre-exponential factor was assumed for the desorption rate constant.[9] The heat of dissociative adsorption has only been directly measured by calorimetry on two systems involving well-defined, single-crystalline oxide surfaces, i.e., H_2O on Fe_3O_4[10] and

H_2O on NiO(111)[11]. This paper adds only the third such report for oxide surfaces, and the first to produce adsorbed formate on NiO(111) besides hydroxyls.

Catalysts based on nickel oxides are of great importance in many chemical and environmental applications, such as steam reforming of methane and biomass conversions.[12-13] Previously, the adsorption and dissociation of HCOOH on (2×2)-NiO(111) thin films grown on Ni(111) were experimentally studied by TPD and infrared reflection adsorption spectroscopy (IRAS).[14-18] It was found that HCOOH dissociatively adsorbs above 160 K on (2×2)-NiO(111) to form adsorbed formate ($HCOO_{ad}$) and adsorbed H (which binds to a surface lattice O to make a surface hydroxyl, -OH), where the $HCOO_{ad}$ and -OH species were identified by IRAS. $HCOO_{ad}$ and -OH were found to be stable on (2×2)-NiO(111)/Ni(111) surface until 320 K but undergo further reactions to form H_2 gas plus CO_2 gas (dehydrogenation path, TPD peaks at ~340, 390, and 520 K) and H_2O gas plus + CO gas (dehydration path, with TPD peaks at ~415 and 520 K).[17] We report here the first experimental measurement of the energy of the dissociative adsorption of formic acid on (2×2)-NiO(111) at 300 K by calorimetry. The differential heat of adsorption decreases with HCOOH coverage from 202 kJ/mol to 99 kJ/mol at saturation coverage (0.25 ML). The integral heat is 153 kJ/mol at saturation, which is ~36 kJ/mol higher than the integral heat of HCOOH dissociatively adsorbed on clean Ni(111) forming adsorbed bidentate formate and adsorbed hydrogen.[8] We also employed DFT to calculate the energies of the reaction and compare these to the calorimetric results to validate their energy accuracies. These results add substantially to our limited knowledge of the energy and structure of surface formate groups on oxide surfaces.

Experimental Methods

The experiments were performed in an ultrahigh vacuum (UHV) chamber (base pressure <2 × 10^{-10} mbar), designed for single-crystal adsorption calorimetry (SCAC) and surface analysis, as described previously.[19-20] Briefly, the chamber is equipped with low-energy electron diffraction (LEED), Auger electron spectroscopy (AES), X-ray photoelectron spectroscopy

(XPS), low-energy ion scattering spectroscopy (LEIS), a quadrupole mass spectrometer (QMS) and a liquid-nitrogen-cooled quartz crystal microbalance (QCM).

The Ni(111) sample used here is a 1 μm thick single-crystal foil, supplied by Jacques Chevallier at Aarhus University in Denmark and the surface was cleaned by cycles of Ar^+ ion sputtering and annealing. A detailed description of the experimental principles and implementation of the molecular beam flux, sticking probability, and heat measurements can be found elsewhere.[19-21] Before each calorimetry experiment, the clean Ni(111) was oxidized with a saturation exposure of O_2 (1×10^{-6} torr for 200 seconds) at 300 K, leading to an epitaxial NiO(111) film whose thickness is 3 or 4 bilayers.[22-25] As described before,[11] this gives a hydroxyl-free, octapolar reconstructed (2×2)-NiO(111) surface. Subsequently, the freshly prepared NiO(111) surface was exposed to a pulsed molecular beam of HCOOH at 300 K, and the adsorption heat and sticking probability were measured simultaneously. The beam was created by expanding ~2 mbar of HCOOH through a microchannel array and then collimated through a series of five liquid nitrogen cooled orifices, and chopped into 102 ms pulses every 5 s with a rotating chopper blade. The microchannel array was heated and kept at 360 K to reduce gas-phase dimerization to less than 1%.[26] The sticking probability was measured employing the King and Wells method,[27] whereby a QMS, non-line-of-sight to the sample, measured the transient increase in the background pressure of $HCOOH_g$ (m/e = 46) in the chamber versus time. We define the coverage of HCOOH molecules which adsorb onto the surface permanently in units of monolayers (ML) where 1 ML = 1.33×10^{19} atoms/m^2, the density of O atoms in a (hypothetically) unreconstructed NiO(111) surface[24]. A typical dose is 0.009 ML (~1.5×10^{12} molecules within the beam diameter of ~4 mm) per HCOOH pulse.

Theoretical Methods

We have also performed density functional theory (DFT) calculations to supplement and support our experiments. Using the Vienna *ab-initio* Software Package (VASP)[28-30] we simulated the dissociative adsorption of HCOOH on NiO (111) in six different configurations

known from previous studies[11] as shown in Figure 3. Based on our previous study of dissociative adsorption of D_2O on this same NiO surface,[11] we have studied the HCOOH adsorption on both: the oxygen- and metal-terminated (2×2) octopolar surfaces of NiO(111), denoted as O-octo and M-octo, which are energetically most favored at preparation conditions of our experiment.[11] Only a single pair of O and Ni exposed sites are available within the (2×2) unit cell of each octopolar surface, which limits the saturated adsorption to a single HCOOH per (2×2) cell, which we refer to as 0.25 ML coverage. Subsequently, we have studied HCOOH adsorption under 1/16, 1/8, 3/16 and at 1/4 ML coverages using any the four equivalent adsorption sites within our (4×4) simulation cell.

Our model systems are symmetric stoichiometric NiO slabs six layers of nickel atoms thick that are separated by at least 15Å of vacuum in the *z* direction and they are periodic in the *xy* plane (using a 2×2 supercell and 2x2 Γ-centered *k*-point mesh). We have used the spin-polarized PBE exchange-correlation functional[31] with a Hubbard U (+U) correction[32] of 6.45 eV on Ni atoms to account for on-site correlation effects, and we note that this level of theory has been used successfully for similar problems in the literature.[11, 33-35] We have also tested the effect of other exchange-correlation functionals commonly employed in catalysis such as RPBE[36] and BEEF-vdW.[37]

We model the core electrons of carbon, nickel, and oxygen atoms with projector augmented wave (PAW) pseudopotentials from the VASP library, notably not using the "soft" option for C or O.[38] We employ a plane wave basis with a cutoff of 550 eV with a full FFT-grid setting to accurately describe valence electrons. The positions of all atoms within the unit cell were relaxed until the force on each atom was less than 0.02 eV*Å^{-1}. Our surfaces, including for structures with adsorbed HCOOH, readily adopt the AFM-type II antiferromagnetic ordering along {111} direction, layers of Ni-ions with alternating sign and with absolute value of magnetic moments of ~1.7 μ_B per Ni atom.

The heat of adsorption q is defined for the experimental measurements as the negative of the enthalpy change upon adsorption (ΔH). We calculate the theoretical integral heat of

adsorption as the sum of the changes in electronic energy at T=0 K (ΔE_{DFT}), zero-point energy (ΔE_{ZPE}), harmonic heat capacity energies ($C\Delta T$) and change in the pressure-volume term ($\Delta(PV) = -PV_{gas} = -RT$) when a formic acid molecule adsorbs (and dissociates in this case) on the catalyst surface:

$$q = -\Delta H = -[(E_{DFT} + ZPE + C\Delta T)_{Ads.+surf.} - E_{Clean} - (E_{DFT} + ZPE + C\Delta T)_{HCOOH}] + RT$$

Here "Ads.+surf." refers to the combined system of catalyst with bound adsorbate, "Clean" refers to the pristine catalyst surface, and "HCOOH" refers to the gas phase formic acid molecule. The sign convention here matches experiment. We assume that the vibrations within the catalyst surface itself are only perturbed slightly by the adsorbate, so we do not consider the contribution of atoms within the oxide surface towards the zero-point energy or harmonic heat capacity. The contributions from adsorbed and gas-phase vibrations almost exactly cancel in all cases, as shown in the Table S2 of Supporting Information (SI).

Experimental Results

Sticking Probability

The short-term and long-term sticking probabilities of HCOOH adsorbing on (2×2)-NiO(111) were measured at 300 K, as shown in Figure 1. The short-term sticking probability (S_{102ms}) is the probability that a gas molecule strikes the sample surface, sticks, and remains at least throughout the time window of our heat measurement (i.e., the first 102 ms). This is used to calculate the number of moles of gas-phase reactant that contribute to the measured heat of adsorption. The long-term sticking probability (S_∞) is the probability that a gas molecule strikes the sample surface, sticks, and remains until the next gas pulse starts ~5 s later, which is used to calculate the adsorbate coverage remaining at the start of the next gas pulse. The long-term sticking probability starts at ~0.86, then quickly increases to ~0.97 and keeps almost unity until ~0.23 ML, where it starts to drop sharply and reaches 0 at ~0.25 ML. The short-term sticking probability follows a very similar trend, but stops dropping at a value of ~0.5 for the saturated adlayer at 0.25 ML. This indicates that ~50% of HCOOH gas molecules in each

pulse transiently adsorb on the saturated surface, but desorb again slowly before the next pulse arrives. The saturation coverage of 0.25 ML is consistent with one HCOOH molecule adsorbing (dissociatively) per unit cell on the p(2×2) octopolar surface structure of NiO(111) studied here.

Heat of Adsorption

In this paper, we define the term *heat of adsorption* as the negative of the differential standard molar enthalpy change for the adsorption reaction, with the gas and the sample surface being at the same temperature. As described previously, this requires a small correction on the gas temperature compared to the actual experimental molecular beam conditions.[21]

According to the literature,[14-18] HCOOH is known to dissociatively adsorb on (2×2)-NiO(111)/Ni(111) at 300 K, forming $HCOO_{ad}$ and H_{ad} (which binds to a lattice O, so it forms a surface –OH). Figure 2 shows the measured differential heat of adsorption vs HCOOH coverage until saturation at ~0.25 ML. The differential heat drops almost linearly with coverage from an initial value of ~202 kJ/mol down to a final value of ~99 kJ/mol at the saturated coverage of 0.25 ML. The integral heat is 153 ± 3 kJ/mol at 0.25 ML (the error here is the run-to-run standard deviation, associated with run-to-run errors in the absolute heat-detector calibration factor). This integral heat is ~36 kJ/mol higher than that for HCOOH dissociative adsorption on clean Ni(111) forming adsorbed bidentate formate and adsorbed hydrogen.[8] After saturation, HCOOH molecules continue to adsorb with S_{102ms} = ~0.5, but desorb again before the next gas pulse (see Figure 1). The heat value for this transiently-adsorbed HCOOH after saturation is 99 ± 3 kJ/mol. The red line in Figure 2 is the best fit to the differential heat data points and has and y-intercept of 202 kJ/mol and a slope of -399 kJ/mol/ML.

We also measured the heat of adsorption at 100 K, shown as Figure S1 in SI, where HCOOH molecularly adsorbs on (2×2)-NiO(111)/Ni(111) according to the literature.[14, 17] The differential heat of adsorption is initially ~90 kJ/mol, and keeps almost constant until ~0.14 ML. That initial heat is ~11 kJ/mol higher than the initial heat of HCOOH molecularly adsorbed on Ni(111),[8] indicating that HCOOH molecularly adsorbs on NiO(111) more strongly than on Ni(111). After

0.14 ML, the heat decreases quickly to ~55 kJ/mol at ~0.25 ML and more slowly to ~51 kJ/mol at ~0.5 ML, and finally remains constant at 50.4 ± 2.3 kJ/mol beyond 0.5 ML, where the multilayers of formic acid are built up on surface. This final heat is consistent with the heat of adsorption of multilayer formic acid on Pt(111)[7] and Ni(111)[8] reported by this group previously. The sticking probability at 100 K was near unity at all coverages.

Theoretical Results

Calculated Energetics of HCOOH Dissociative Adsorption

We have considered six different adsorption configurations for the formate and H products of HCOOH dissociation, spanning both O-octo and M-octo surface terminations using DFT+U method (see also Theoretical Methods), as shown in Figure 3. The final optimized structures of adsorbed $HCOO_{ad}$ were found to bind to the surface through one or both of its oxygens. We borrow terminology from Ref. [15]: in the "bidentate" configuration, both oxygens in $HCOO_{ad}$ bind to one nickel atom, in "monodentate" configurations one oxygen in $HCOO_{ad}$ binds to a nickel atom while the other forms a hydrogen bond to the dissociated hydrogen, and in "bridging" configurations each oxygen in $HCOO_{ad}$ binds to different nickel atoms. "Hex-bridging" follows the same principles as "bridging," but binds to tow upmost nickel atoms in a symmetric fashion. In all cases, the H product was found to form OH group at the nearby surface O^{2-} of the NiO lattice, confirming the basic character of the oxide surface's oxygen anion, as seen previously for MgO surfaces.[39]

First, we highlight the similarity between the most stable configurations' energetics from Figure 3 for each termination at the low-coverage limit: -226 kJ/mol (O-octo hex-bridging), -195 kJ/mol (M-octo bridging) and the experimentally measured value in the -202 kJ/mol. Both calculated values are relatively close to experimentally measured value, which suggests that we are describing the dominant interactions between the $HCOO_{ad}$, H_{ad}, and (2×2)-NiO(111) appropriately. Additionally, both types of surface terminations have similar adsorption energetics and therefore their simultaneous presence in experimental samples cannot be eliminated as a

possibility by comparison to the experimental heats. This is also a test of the calculated surface energies of these two surface terminations when clean (before adsorption), which we found to be identical within expected error bars of the calculation.[11] Another important finding from our calculations is that the bridging geometries for $HCOO_{ad}$ are always energetically preferred over monodentate and bidentate type bonding. Additionally, we also demonstrate in Table S1 in SI that the vibrational eigenmode frequencies of bridge-bonded formate structures for both terminations calculated with PBE+U compare favorably to previous experimental values using infrared spectroscopy.[16]

Next, in Figure 4, we show the calculated integral adsorption enthalpy (ΔH) on both the O-octo and M-octo terminations as function to coverage up to ¼ ML. The O-octo surface (shown in red) clearly adsorbs $HCOO_{ad}$ and H_{ad} more strongly than the M-octo surface (shown in blue) for all bonding modes. For the O-octo surface, the calculated integral ΔH is constant or an increasing function of the coverage which is in contrast with the strong decrease seen in the experimental calorimetry results shown in Figure 2. The M-octo surface shows configurations where the calculated integral ΔH is a decreasing function of the coverage and generally much closer to the experimental line at all considered coverages. Introducing a metallic Ni(111) support below the oxide film or mixed adsorbate configurations at ¼ ML did not change the calculated trends for the O-octo surface (shown as Figure S4 of SI). Calculations at coverages up to ¼ ML are therefore essential in order to capture the adsorption energetics on NiO(111) surfaces. Furthermore, DFT also shows that dissociative adsorption is much less favorable at coverages above ¼ ML due to unavailability of free adsorption sites which also agrees with saturation observed in our experiment.

Lastly, we have also tested the influence of changing the Hubbard (+U) parameter and the exchange-correlation functional on our results. We found no qualitative difference in the relative stabilities of structures for any of the cases tested, as shown in Figure S2 of the SI. Increasing the value of the U-parameter leads to weaker adsorption, while decreasing the U-parameter leads to increasing the adsorption in agreement with our previous study for D_2O adsorption on this

same surface.[11] We further show that changing the exchange-correlation functional does not substantially alter calculated adsorbate-adsorbate interactions in Figure S3 of the SI.

Discussion

Discussion of Theory vs. Experiment

We find good agreement between theory and experiment at low coverages of dissociatively adsorbed HCOOH, where the experimentally observed value for differential heat of adsorption is consistent with adsorption energetics calculated at either O-octo (2×2) or M-octo (2×2) surfaces. The largest decrease in heat of adsorption with coverage is observed for a bridge-bonded geometry of formate on the M-octo surface, where the integral heat drops from 195 kJ/mol at low coverage to 180 kJ/mol at 0.25 ML. This 15 kJ/mol decrease indicates that repulsive electronic adsorbate-adsorbate interactions are present in this system, but do not account for the full ~45 kJ/mol decrease shown in Figure 2. Adsorbate-adsorbate repulsion for these molecules typically arises either due to dipole-dipole interactions or substrate mediated interactions. For the O-octo surface, we have tested separately the effect of mixed adsorption modes and the effect of Ni(111) metallic support, both of which had only small effects on the adsorption energy at high coverage (See Figure S4). Furthermore, the calculated trends were independent of the choice of exchange-correlation functional or choice of Hubbard-U (see Figure S2).

The discrepancy of DFT predictions with experimental measurement on the other hand can be more simply explained if we would allow for the presence of both types of terminations on the clean surface of our experimental sample. In this picture, the mixture of O-octo and M-octo surfaces would be exposed to the adsorption of HCOOH molecules. At low coverage, the most energetically favorable hex-bridging geometry on the O-octo surface ($-\Delta H$=226 kJ/mol) would dominate the adsorption. This assumes that the un-dissociated HCOOH is mobile on the surface and finds sites with the lowest barrier and are also the most exothermic for dissociation assuming BEP scaling relations.[40] Only after all available O-octo sites are filled, the M-octo sites could adsorb preferentially in the bridge geometry ($-\Delta H$=180 kJ/mol). For some fraction f of the

surface area being O-octo (and thus 1-f as M-octo), the integral -ΔH at ¼ ML would therefore equal $f * 226 + (1 - f) * 180$ kJ/mol. For a 50/50 mixture of O-octo to M-octo, the final integral heat would drop from 226 to 203 kJ/mol, or 23 kJ/mol lower ΔH relative to low coverage. Higher area fractions of M-octo would therefore effectively lower the adsorption energetics at high coverage, closer to measured ~45 kJ/mol decrease.

Conclusions

In this study, we have used calorimetric measurements and density functional theory to examine the energetics of formic acid dissociative adsorbed on a (2×2)-NiO(111) surface. They agree with each other quite well at the limit of low coverage of adsorbates. However, we find that experiments show a clear downward trend in adsorption energies at higher coverages, while calculations suggest this is not a straightforward case of electronic adsorbate-adsorbate repulsion. We inferred that the decreased binding strength may be indicative of heterogeneous adsorption at the (2×2)-NiO(111) surface, with respect to oxygen- and metal-termination both being present on the starting surface, and/or binding site differences. We confirm that all calculated configurations considered show similar energetics and vibrational spectra at low coverage (see Table S1). These findings provide a more detailed understanding of the system studied, and underscore the importance of combined experimental and DFT-based approaches to understanding the catalysis of transition-metal oxides.

Supporting Information. Differential heat of molecular adsorption of HCOOH on (2×2)-NiO(111) at 100 K measured by calorimetry; comparison of the calculated adsorption energies at 0 K and a coverage of 1/16 ML with different exchange-correlation functionals and the Hubbard (+U) term on Ni 3d orbitals; comparison of the calculated integral heats of adsorption at two different coverages (1/4 ML and 1/16 ML) using different exchange-correlation functionals; same as Figure 4 with extra points considering an O-octo surface supported on Ni(111), and mixing of various adsorbate modes on O-octo; same as Figure

3, but including the top view of the adsorbed HCOOH; vibrational eigenmodes observed in experiment (Ref. 16) and calculated using DFT; thermochemistry corrections used to convert between calculated electronic energies and binding energies at a coverage of 1/16 ML using PBE+U.

Acknowledgements

Support from the Office of Basic Energy Sciences of the U.S. Department of Energy to the SUNCAT Center for Interface Science and Catalysis at SLAC/Stanford is gratefully acknowledged. A.D. and M.B. would like to acknowledge the use of the computer time allocation for the "Computational search for highly efficient 2d & 3d nano-catalysts for water splitting" at the National Energy Research Scientific Computing Center, a DOE Office of Science User Facility supported by the Office of Science of the U.S. Department of Energy under Contract No. DE-AC02-05CH11231.

Figures and captions

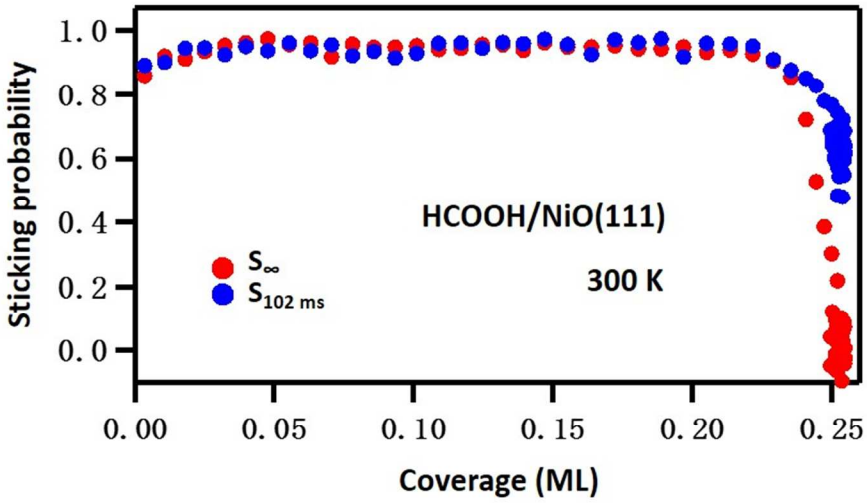

Figure 1. Long-term (S_∞: in red) and short-term ($S_{102\ ms}$: in blue) sticking probabilities of HCOOH on (2×2)-NiO(111) as a function of the total HCOOH coverage that adsorbed at 300 K. One ML is defined as 1.33×10^{19} adsorbed HCOOH molecules per m^2, in this case being dissociatively adsorbed.

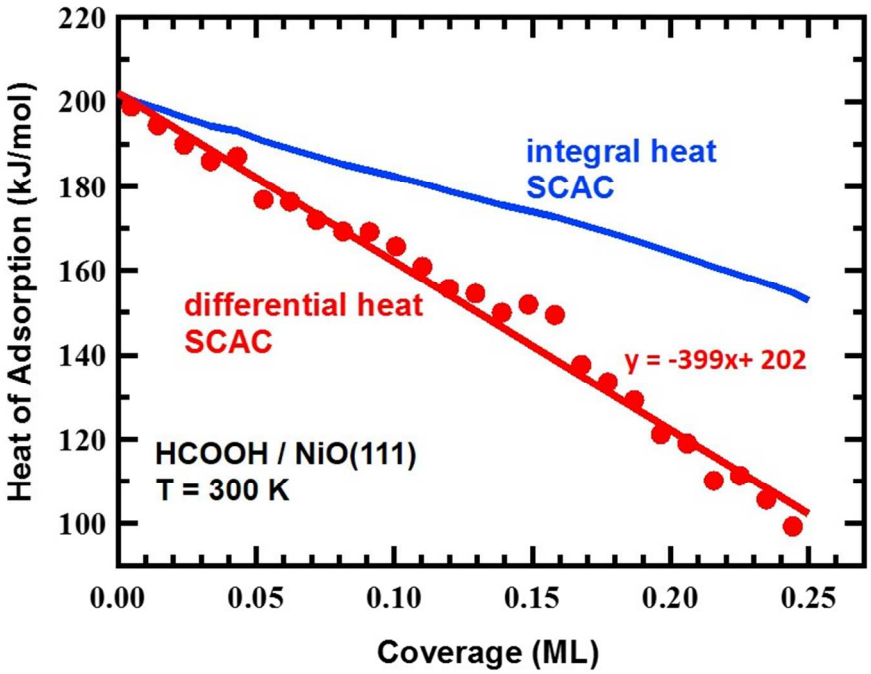

Figure 2. Differential heat of dissociative adsorption (-ΔH) of HCOOH on (2×2)-NiO(111) at 300 K versus the total coverage of dissociatively adsorbed HCOOH measured by calorimetry (SCAC, red data points). The red line shown is the best linear fit to the differential heat data points and has a y-intercept of 202 kJ/mol and a slope of -399 (kJ/mol)/ML. The integral heat for the dissociatively adsorbed HCOOH is also plotted versus HCOOH coverage (the blue curve), giving 153 ± 3 kJ/mol at 0.25 ML.

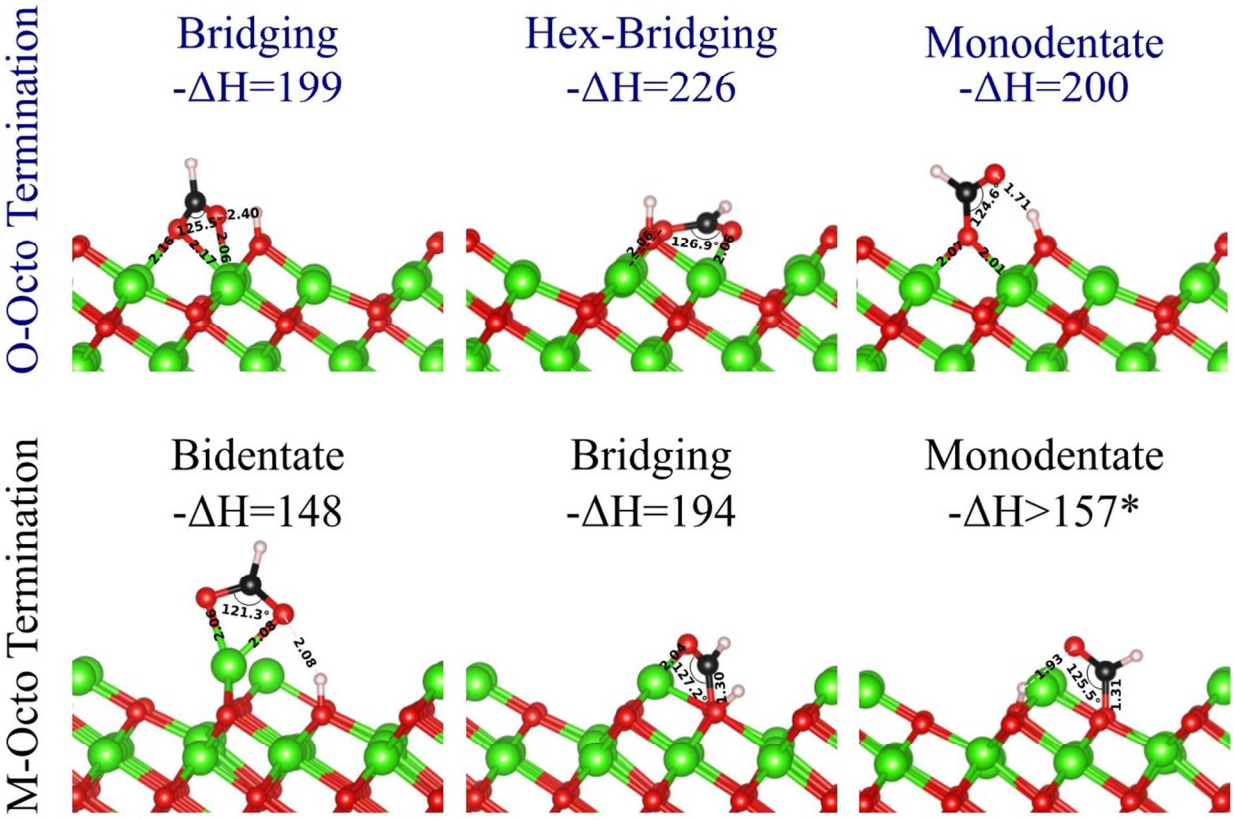

Figure 3. DFT calculated integral heats of dissociative adsorption of HCOOH (-ΔH, in kJ/mol) and resulting optimized surface structures for different adsorption configurations of formate (Bidentate, Bridging, Hex-Bridging, Monodentate) at low coverage. Calculated adsorption energies (in kJ/mol) shown in the lower-left for both the O- and M- terminated (O-octo and M-octo) (2×2)-NiO(111) surfaces, at 1/16 ML coverage, obtained using PBE+U DFT. *We note that in our calculations, the monodentate adsorption configuration on M-octo surfaces is only stable at 0.25 ML coverage. At lower coverages, it is metastable, and reverts to a bridging configuration. The structural parameters of the adsorbate are also shown. For more detailed view and complete geometries, see Figure S5 in SI.

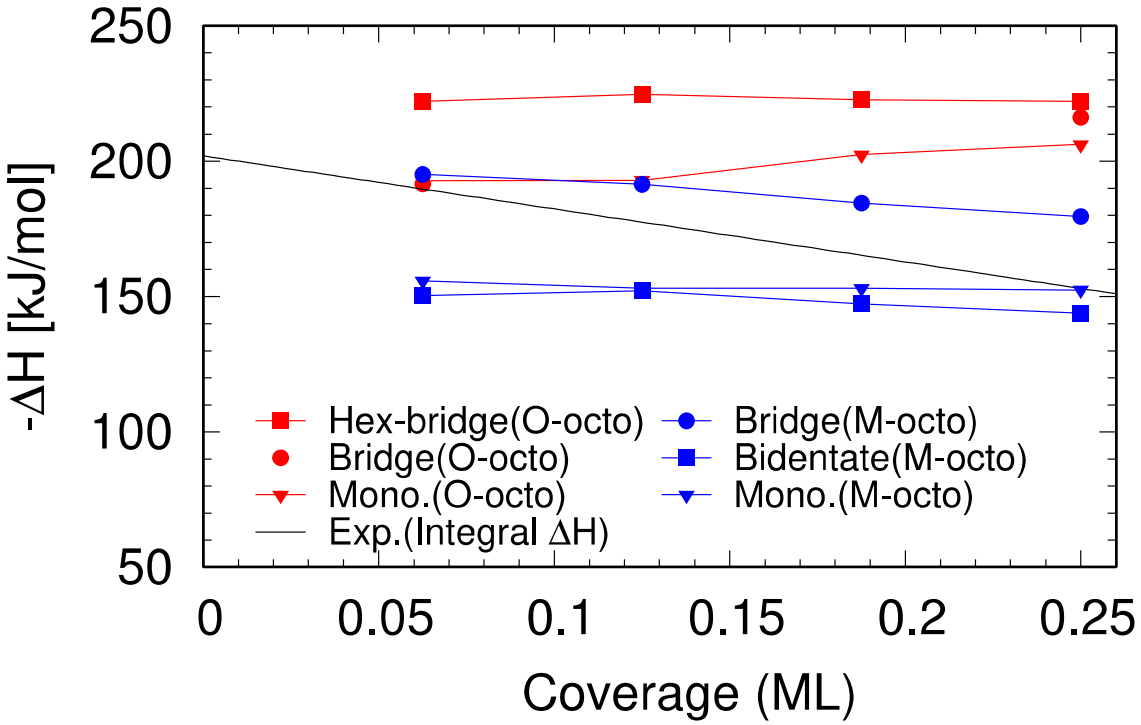

Figure 4: Calculated ΔH of adsorption at 0 K for all possible types of dissociative HCOOH adsorption as function of HCOOH coverage from 1/16 ML to 1/4 ML on O-octo (red symbols) and M-octo (blue symbols). The experimental measurement at 300 K is also shown for comparison (solid black line). Due to computational limitations, here we used a less expensive 400 eV cut-off for our plane wave basis together with softer potentials for oxygen and carbon. These results deviate less than 3 kJ/mol from more accurate values obtained at 550 eV plane wave cut off at low coverage.

References

1. Singh, A. K.; Singh, S.; Kumar, A., Hydrogen Energy Future with Formic Acid: A Renewable Chemical Hydrogen Storage System. *Catal. Sci. Technol.* **2016**, *6*, 12-40.
2. Mellmann, D.; Sponholz, P.; Junge, H.; Beller, M., Formic Acid as a Hydrogen Storage Material - Development of Homogeneous Catalysts for Selective Hydrogen Release. *Chem. Soc. Rev.* **2016**, *45*, 3954-3988.
3. Grabow, L. C.; Gokhale, A. A.; Evans, S. T.; Dumesic, J. A.; Mavrikakis, M., Mechanism of the Water Gas Shift Reaction on Pt: First Principles, Experiments, and Microkinetic Modeling. *J. Phys. Chem. C* **2008**, *112*, 4608-4617.
4. Flaherty, D. W.; Yu, W.-Y.; Pozun, Z. D.; Henkelman, G.; Mullins, C. B., Mechanism for the Water–Gas Shift Reaction on Monofunctional Platinum and Cause of Catalyst Deactivation. *J. Catal.* **2011**, *282*, 278-288.
5. Catapan, R. C.; Oliveira, A. A. M.; Chen, Y.; Vlachos, D. G., DFT Study of the Water–Gas Shift Reaction and Coke Formation on Ni(111) and Ni(211) Surfaces. *J. Phys. Chem. C* **2012**, *116*, 20281-20291.
6. Barth, J. V.; Costantini, G.; Kern, K., Engineering Atomic and Molecular Nanostructures at Surfaces. *Nature* **2005**, *437*, 671-679.
7. Silbaugh, T. L.; Karp, E. M.; Campbell, C. T., Energetics of Formic Acid Conversion to Adsorbed Formates on Pt(111) by Transient Calorimetry. *J. Am. Chem. Soc.* **2014**, *136*, 3964-3971.
8. Zhao, W.; Carey, S. J.; Morgan, S. E.; Campbell, C. T., Energetics of Adsorbed Formate and Formic Acid on Ni(111) by Calorimetry. *J. Catal.* **2017**, *352*, 300-304.
9. Campbell, C. T.; Sellers, J. R. V., Enthalpies and Entropies of Adsorption on Well-Defined Oxide Surfaces: Experimental Measurements. *Chem. Rev.* **2013**, *113*, 4106-4135.
10. Dementyev, P.; Dostert, K.-H.; Ivars-Barceló, F.; O'Brien, C. P.; Mirabella, F.; Schauermann, S.; Li, X.; Paier, J.; Sauer, J.; Freund, H.-J., Water Interaction with Iron Oxides. *Angew. Chem. Int. Ed.* **2015**, *54*, 13942-13946.
11. Zhao, W.; Bajdich, M.; Carey, S.; Vojvodic, A.; Nørskov, J. K.; Campbell, C. T., Water Dissociative Adsorption on Nio(111): Energetics and Structure of the Hydroxylated Surface. *ACS Catal.* **2016**, *6*, 7377-7384.
12. Diskin, A. M.; Cunningham, R. H.; Ormerod, R. M., The Oxidative Chemistry of Methane over Supported Nickel Catalysts. *Catal. Today* **1998**, *46*, 147-154.
13. Zhu, T.; Flytzani-Stephanopoulos, M., Catalytic Partial Oxidation of Methane to Synthesis Gas over Ni–CeO_2. *Appl. Catal. A* **2001**, *208*, 403-417.
14. Bandara, A.; Kubota, J.; Wada, A.; Domen, K.; Hirose, C., Adsorption and Decomposition of Formic Acid (DCOOD) on NiO(111) and Ni(111) Surfaces Probed by SFG. *Appl. Phys. B* **1999**, *68*, 573-578.

15. Bandara, A.; Kubota, J.; Wada, A.; Domen, K.; Hirose, C., Adsorption and Reactions of Formic Acid on (2×2)-NiO(111)/Ni(111) Surface. 2. IRAS Study under Catalytic Steady-State Conditions. *J. Phys. Chem. B* **1997**, *101*, 361-368.
16. Bandara, A.; Kubota, J.; Wada, A.; Domen, K.; Hirose, C., Adsorption and Reactions of Formic Acid on (2×2)-NiO(111)/Ni(111) Surface. 1. TPD and IRAS Studies under Ultrahigh Vacuum Conditions. *J. Phys. Chem.* **1996**, *100*, 14962-14968.
17. Bandara, A.; Kubota, J.; Wada, A.; Domen, K.; Hirose, C., Adsorption and Decomposition of Formic Acid on the NiO(111)-p(2 × 2) Surface: TPD and Steady State Kinetics Studies. *Surf. Sci.* **1996**, *364*, L580-L586.
18. Matsumoto, T.; Bandara, A.; Kubota, J.; Hirose, C.; Domen, K., Adsorption and Reaction of Formic Acid on a (2 × 2) NiO(111)/Ni(111) Surface. 3. IRAS Studies on the Characterization of Reaction Sites Using CO and the Behavior of Surface Hydroxyl Species. *J. Phys. Chem. B* **1998**, *102*, 2979-2984.
19. Ajo, H. M.; Ihm, H.; Moilanen, D. E.; Campbell, C. T., Calorimeter for Adsorption Energies of Larger Molecules on Single Crystal Surfaces. *Rev. Sci. Intrum.* **2004**, *75*, 4471-4480.
20. Lew, W.; Lytken, O.; Farmer, J. A.; Crowe, M. C.; Campbell, C. T., Improved Pyroelectric Detectors for Single Crystal Adsorption Calorimetry from 100 to 350 K. *Rev. Sci. Intrum.* **2010**, *81*, 024102.
21. Lytken, O.; Lew, W.; Harris, J. J. W.; Vestergaard, E. K.; Gottfried, J. M.; Campbell, C. T., Energetics of Cyclohexene Adsorption and Reaction on Pt(111) by Low-Temperature Microcalorimetry. *J. Am. Chem. Soc.* **2008**, *130*, 10247-10257.
22. Langell, M. A.; Nassir, M. H., Stabilization of NiO(111) Thin Films by Surface Hydroxyls. *J. Phys. Chem.* **1995**, *99*, 4162-4169.
23. Norton, P. R.; Tapping, R. L.; Goodale, J. W., A Photoemission Study of the Interaction of Ni(100), (110) and (111) Surfaces with Oxygen. *Surf. Sci.* **1977**, *65*, 13-36.
24. Okazawa, T.; Nishizawa, T.; Nishimura, T.; Kido, Y., Oxidation Kinetics for Ni(111) and the Structure of the Oxide Layers. *Phys. Rev. B* **2007**, *75*, 033413.
25. Kitakatsu, N.; Maurice, V.; Hinnen, C.; Marcus, P., Surface Hydroxylation and Local Structure of NiO Thin Films Formed on Ni(111). *Sur. Sci.* **1998**, *407*, 36-58.
26. Coolidge, A. S., The Vapor Density and Some Other Properties of Formic Acid. *J. Am. Chem. Soc.* **1928**, *50*, 2166-2178.
27. King, D. A.; Wells, M. G., Molecular Beam Investigation of Adsorption Kinetics on Bulk Metal Targets: Nitrogen on Tungsten. *Surf. Sci.* **1972**, *29*, 454-482.
28. Kresse, G.; Hafner, J., Ab *Initio* Molecular Dynamics for Liquid Metals. *Phys. Rev. B* **1993**, *47*, 558-561.
29. Kresse, G.; Furthmüller, J., Efficiency of ab-initio Total Energy Calculations for Metals and Semiconductors Using a Plane-Wave Basis Set. *Comp. Mat. Sci.* **1996**, *6*, 15-50.
30. Kresse, G.; Furthmüller, J., Efficient Iterative Schemes for ab initio Total-Energy Calculations Using a Plane-Wave Basis Set. *Phys. Rev. B* **1996**, *54*, 11169-11186.
31. Perdew, J. P.; Burke, K.; Ernzerhof, M., Generalized Gradient Approximation Made Simple. *Phys. Rev. Lett.* **1996**, *77*, 3865-3868.

32. Dudarev, S. L.; Botton, G. A.; Savrasov, S. Y.; Humphreys, C. J.; Sutton, A. P., Electron-Energy-Loss Spectra and the Structural Stability of Nickel Oxide: an LSDA+U Study. *Phys. Rev. B* **1998**, *57*, 1505-1509.
33. Doyle, A. D.; Bajdich, M.; Vojvodic, A., Theoretical Insights to Bulk Activity Towards Oxygen Evolution in Oxyhydroxides. *Catal. Lett.* **2017**, *147*, 1533-1539.
34. Tkalych, A. J.; Yu, K.; Carter, E. A., Structural and Electronic Features of β-$Ni(OH)_2$ and β-NiOOH from First Principles. *J. Phys. Chem. C* **2015**, *119*, 24315-24322.
35. Gautier, S.; Steinmann, S. N.; Michel, C.; Fleurat-Lessard, P.; Sautet, P., Molecular Adsorption at Pt(111). How Accurate Are DFT Functionals? *Phys. Chem. Chem. Phys.* **2015**, *17*, 28921-28930.
36. Hammer, B.; Hansen, L. B.; Nørskov, J. K., Improved Adsorption Energetics within Density-Functional Theory Using Revised Perdew-Burke-Ernzerhof Functionals. *Phys. Rev. B* **1999**, *59*, 7413-7421.
37. Wellendorff, J.; Lundgaard, K. T.; Møgelhøj, A.; Petzold, V.; Landis, D. D.; Nørskov, J. K.; Bligaard, T.; Jacobsen, K. W., Density Functionals for Surface Science: Exchange-Correlation Model Development with Bayesian Error Estimation. *Phys. Rev. B* **2012**, *85*, 235149.
38. Kresse, G.; Joubert, D., From Ultrasoft Pseudopotentials to the Projector Augmented-Wave Method. *Phys. Rev. B* **1999**, *59*, 1758-1775.
39. Peng, X. D.; Barteau, M. A., Acid-Base Reactions on Model Mgo Surfaces. *Catal. Lett.* **1992**, *12*, 245-253.
40. Wang, S.; Vorotnikov, V.; Sutton, J. E.; Vlachos, D. G., Brønsted–Evans–Polanyi and Transition State Scaling Relations of Furan Derivatives on Pd(111) and Their Relation to Those of Small Molecules. *ACS Catal.* **2014**, *4*, 604-612.

TOC Graphic: